Defect and Diffusion Forum
ISSN: 1662-9507, Vol. 450, pp 19-30
doi:10.4028/p-xi5kxU

Submitted: 2025-12-22
Revised: 2026-02-23
Accepted: 2026-02-24
Online: 2026-04-15

Condition-Robust Tool Remaining Useful Life Prediction under Highly Variable Milling Conditions

Stefania Ferrisi[1,a*], Sebastian Lang[2,b], Mohamadreza Afrasiabi[2,c], Rosita Guido[1,d], Domenico Umbrello[1,e], Giuseppina Ambrogio[1,f] and Markus Bambach[2,g]

[1]Department of Mechanical, Energetic and Management Engineering, University of Calabria, Ponte P. Bucci, Rende, 87036, CS, Italy

[2]Advanced Manufacturing Lab, ETH Zurich, Zurich, Switzerland

[a*]stefania.ferrisi@unical.it, [b]selang@ethz.ch, [c]afrasiabi@ethz.ch, [d]rosita.guido@unical.it, [e]domenico.umbrello@unical.it, [f]giuseppina.ambrogio@unical.it, [g]mbambach@ethz.ch

*corresponding author

Keywords: milling process, remaining useful life, tool wear, deep learning.

Abstract. Accurate prediction of tool Remaining Useful Life (RUL) is essential for reliable and cost-effective milling, particularly when machining commercially pure titanium (CP-Ti), where tool wear is highly irregular. In industrial practice, continuously varying cutting conditions further complicate tool condition monitoring and life prediction. This paper proposes a vibration-based monitoring framework for RUL prediction under strongly variable milling conditions. A hybrid deep learning model based on CNN–BiLSTM is developed to capture the non-stationary relationship between vibration signals and tool degradation. Performance is compared between a spindle-mounted, non-invasive sensor and a tri-axial accelerometer mounted on the machine table, and the benefit of sensor fusion is assessed. Results show that spindle vibration correlates strongly with tool degradation and achieves predictive performance close to that of multi-sensor configurations, while requiring minimal instrumentation. The proposed approach remains robust under variations in both operating conditions and wear mechanisms, enabling reliable RUL estimation in non-stationary milling environments.

Introduction

Commercially pure Titanium (CP-Ti) is the ideal titanium-based material for medical applications due to its excellent properties in terms of biocompatibility and corrosion resistance. It is widely used for dental and bone implants [1]. Due to the unique attributes of the CP-Ti, such as light weight, hypoallergenicity, and durability, it is also used to make products primarily used in everyday life, including titanium bottles, thermos, kitchen utensils, tea sets, sporting goods, etc [2]. In contrast, several studies have demonstrated that the use of titanium alloy (especially the most used Ti-6Al-4V) might cause some long-term health problems for the patient due to the release of aluminum and vanadium inside the human body [3].

The machinability of titanium presents several challenges, such as its low thermal conductivity, adhesion to the cutting tool, and the significant impact of machining parameters. Titanium is considered one of the hardest-to-machine materials for milling. The chips formed during machining are highly flammable and require adequate safety precautions. For this reason, low cutting speeds, heavy feed rates, and the usage of cutting fluid are recommended for its machining. Titanium is a poor heat conductor, unable to dissipate heat quickly, concentrating it on the cutting edge and surface of the tool. Consequently, the cutting tool undergoes intense wear. Different wear mechanisms may be observed during the milling of CP-Ti material, including adhesive wear, diffusion wear, abrasive wear, and thermal cracking. During adhesive wear, a rapid build-up of agglomerated workpiece material adheres to the cutting edge of the tool [4], thereby generating the so-called built-up edge (BUE) effect. This type of wear changes the shape of the cutting tool, altering its size and preventing efficient chip formation during machining. When working under such conditions, the tool can suffer catastrophic wear, resulting in the breakage of one or more teeth. To avoid these effects, cooling

methods are usually employed [5], although they come with drawbacks such as coolant contamination, increased cost and energy consumption, environmental concerns, and health risks associated with coolant residue [6]. However, Assis et al. [7] demonstrated that dry micro-cutting is feasible at adequate feed rates. Finally, changes in chip formation can increase cutting forces during machining, generate excited vibrations, and increase the temperature of the process, exerting a micro-fatigue loading on the cutting tool and decreasing the tool life [8]. As a result of the complex wear mechanisms and the strong dependence of tool degradation on cutting parameters, the accurate monitoring and prediction of tool wear during CP-Ti machining becomes essential to ensure surface quality, dimensional accuracy, and process sustainability. Khan et al. [9] employed an RSM-based quadratic model for the prediction of flank tool wear, obtaining lower prediction error. Nevertheless, as emerged from the analysis of tool wear progression, several tool degradation effects were exhibited (i.e., BUE, chipping, and notch wear).

With the introduction of smart machines in the industrial context, new approaches to tool wear monitoring primarily rely on indirect signal analyses (e.g., cutting forces, acoustic emissions, vibrations, temperatures). These signals can be acquired with the use of Industrial Internet of Things (IIoT), enabling the collection of sensor data useful for the construction of condition-based monitoring systems. By constructing a predictive model for the end-of-life of industrial assets, manufacturers can plan the budget for replacement or repair, reduce maintenance costs, and maximize resource allocation [10]. The extraction of non-stationary and nonlinear signal characteristics from acquired signals enables the construction of accurate prediction models for tool life. The phase of signal processing for the extraction of meaningful information from sensor data plays a critical role in tool condition monitoring (TCM) [11]. Representative features may be extracted or constructed during the signal processing stage as a compact and informative representation for the monitored variables [12]. Assafo et al. [13] analyzed three cutting force signals and extracted time-domain and multiscale features for the prediction of the remaining useful life (RUL) of cutting tools for a milling process. Guo et al. [14] created a time-frequency feature dataset from a multi-sensor signal acquisition system that consists of seven sensors (including acoustic emission sensor, microphone, and accelerometers). Chen et al. [15] proposed an innovative predictive model for RUL based on a data fusion process through a Graph Neural Network combined with a Transformer.

However, these methods encounter considerable difficulties in real-time implementation due to the high cost and invasiveness of the sensors [16], and in defining a robust model under variable working conditions [17]. The ability of a TCM system mainly relies on the number and type of sensors adopted to monitor the process. This, in turn, involves expensive hardware, which influences the cost of the system [18]. Additionally, to satisfy the industrial environment requirements, there is a need to train the predictive model under a different set of cutting conditions [12].

Despite the significant progress achieved in recent years, the literature highlights that most TCM and RUL prediction strategies still struggle to maintain accuracy and reliability when machining conditions vary. This difficulty becomes even more pronounced in the case of CP-Ti, where the progression of tool wear is highly irregular and difficult to model due to the complex tribological behaviour of this material and the strong influence of cutting parameters on chip formation, adhesion, and thermal load on the cutting edge. To address these limitations, the present work proposes a robust data-driven framework for the prediction of RUL of milling cutting tools during CP-Ti machining, explicitly designed to remain stable under a broad range of machining parameters and under the intrinsic wear variability of this material. An extensive experimental campaign was carried out to support the development and validation of the proposed approach. Vibrational data were collected using two complementary sensing systems: (i) a smart tool holder equipped with an embedded radial acceleration sensor capable of wireless data transmission to a tablet device, providing a non-invasive solution, and (ii) a tri-axial accelerometer mounted on the machine table, which offers a full three-axis acquisition but introduces a more invasive installation due to the need for cabling and fixturing. The experimental plan includes variations in machining parameters both between different new tools and dynamically applied to the same tool across successive passes, enabling the construction of a heterogeneous dataset that captures diverse and highly irregular degradation patterns typical of CP-

Ti machining. Based on the acquired dataset, prediction models were trained and evaluated to identify the most effective strategy for real-time RUL estimation. The models were first assessed using the signals from each sensor independently, allowing the standalone predictive capability of the smart spindle and the table-mounted accelerometer to be compared. A further evaluation was then conducted by combining the signals from both sensing systems to understand whether sensor fusion could enhance robustness and accuracy. This comparative analysis provides insights into the specific contribution of each sensor placement and highlights the potential benefits of leveraging heterogeneous vibration sources for reliable tool-life prediction.

The remainder of the paper is organized as follows. Section Experimental Setup describes materials, tools, and sensors used for the experimental campaign and the strategy adopted for the setting of variable cutting conditions. Section Methodology provides background about the algorithms adopted in this study. The results obtained are analyzed and compared in Section Results and Discussion, where the performance of the different approaches is critically assessed. Finally, Section Conclusions and Future Work summarizes the main findings of the study and outlines potential directions for future research.

Experimental Setup

An experimental campaign was conducted over a period of three months with the objective of acquiring a heterogeneous dataset with varying cutting conditions. The DMG Mori NMV 5000 DCG, a 5-axis Machine Tool (MT), was employed for the milling operations on a CP-Ti workpiece with dimensions 270 mm × 270 mm × 26 mm. Carbide end mills with a diameter of 10 mm and unequal helices were used. Table 1 provides the specifications of the machine tool, workpiece, and cutting tools adopted in this study.

Table 1. Specifications of the machine tool, workpiece, and cutting tools adopted for the experimentation.

Component	Specification	Value
Machine tool		DMG Mori NMV 5000 DCG
		Vertical milling machine
	Travel dimension	730 mm (X-axis), 510 mm (Y-axis), 510 mm (Z-axis)
	Tool capacity	31-tool automatic tool changer (ATC)
	Spindle speed	Up to 1200 rpm
	CNC control	FANUC 31iA5
Milling cutter		Carbide end mill
	Helix angles	A= 40°, B= 42°
	Cutting diameter	10 mm
	Number of cutting edges	4
	Bar material	tungsten carbide
	Hardness	HRC72
	Coating	CVD TiCN+Al2O3+TiN
Workpiece		CP-Ti plate
	Size	270 x 270 x 26 mm

The MT was equipped with three sensors for the acquisition of signals and inspection of the cutting tools' condition. In detail, two indirect sensors were installed for the acquisition of real-time vibration signals during milling. The first device is a tri-axial accelerometer (model 356B18 by PCB Piezotronics) installed on the worktable, near the workpiece, enabling the acquisition of vibrations transmitted through the workpiece-machine structure. Data were sampled at a rate of 2048 Hz and collected using a National Instruments NI 9234 Data Acquisition System (DAQ). The second device is the REGO-FIX ToolVibe, a sensory tool holder capable of measuring the radial acceleration of the tool. The data were sampled at 15385 Hz. ToolVibe is a wireless sensor that transmits data to a tablet on a frequency band of 2.4 GHz.

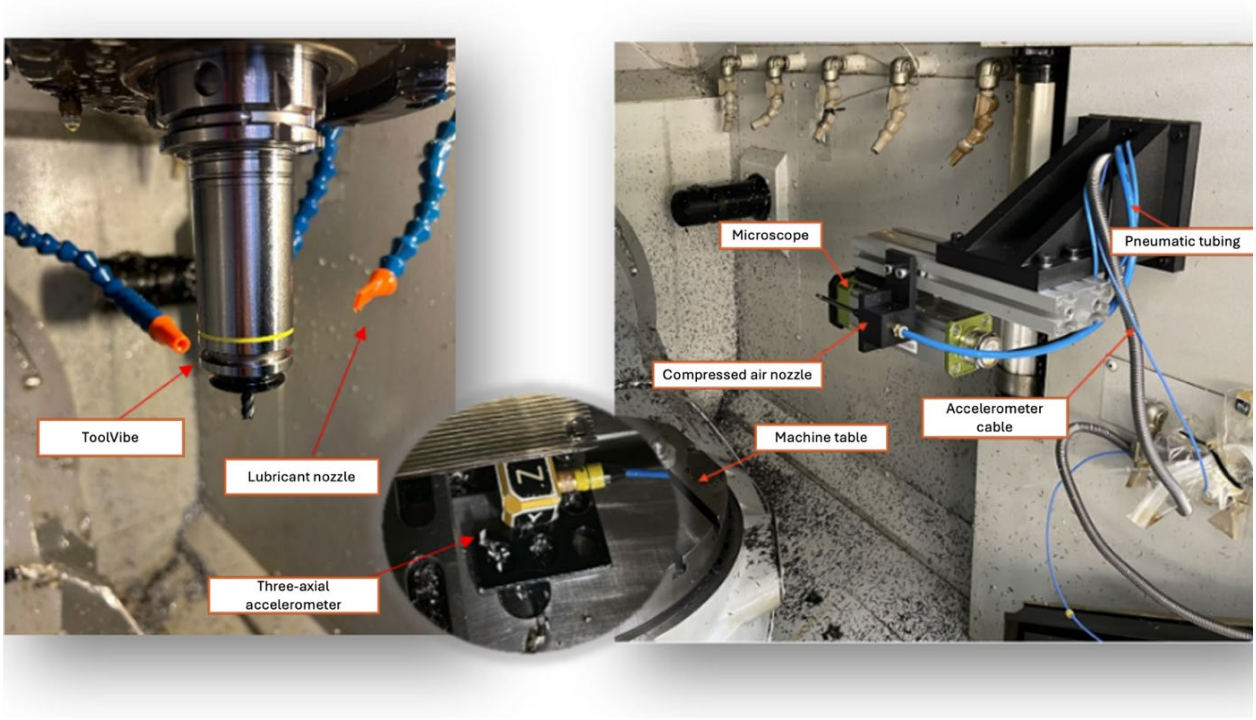

Fig. 1. Sensor configuration adopted during the experimentation.

Unlike the invasive tri-axial accelerometer, which requires wired connections for signal transmission, the ToolVibe system is a non-invasive device, making it more suitable for industrial environments. The third sensor is a direct sensor adopted for the monitoring of the cutting tools' condition after each milling pass. A Dino-Lite AM8917MZTL microscope was installed inside the MT on the right hand side, using a bracket fastening it to the inner wall of the machine with six screws. For protection, the microscope was housed in an Autovimation Salamander M protective casing, while the lens was protected from coolant by a pneumatically actuated cap. The microscope has a resolution of up to 8.0 Megapixels and a magnification set to 140x. The DNX64 Python module was used for controlling it. Finally, a nozzle was installed near the microscope to clear the cutting tool from residual lubricants and material chips before each image acquisition. This nozzle is controlled by an Arduino that controls two solenoid valves connected to the nozzle and the actuators for the microscope cap. A single Python script was used to coordinate machine movements using the FOCAS2 interface as well as data collection and imaging. At the end of each milling pass, the cutting tool reaches the nozzle for cleaning. Then the microscope cap is opened, and the cutting tool reaches the right position for capturing images of the edge, rotating to obtain the four edge images. Fig.1 shows the sensors used during the experimental campaign. Five cutting tools were consumed during the milling process to acquire data, with varying cutting parameter settings. Table 2 illustrates the combination of parameters adopted for each experiment. In addition, a sixth cutting tool was employed in a series of milling operations where the cutting parameters were varied to evaluate the predictive performance of the model under variable conditions. The cutting parameters for these variable experiments were selected using a Sobol quasi-random search [19] within predefined ranges (cutting speed between 25 and 80 m/min, feed between 0.05 and 0.115 mm/tooth, axial depth of cut between 0.6 and 3 mm, radial depth of cut between 0.1 and 5 mm). The experiments were executed in blocks, with each block defined by a fixed radial depth of cut maintained constant until the full depth of the workpiece was machined. After completing a block, a new radial depth of cut was selected for the subsequent block. For each block, the presence of cutting oil was assigned randomly as either yes or no. This approach allowed for the systematic variation of process parameters while ensuring that any potential residual oil on the workpiece could be cleaned between blocks, minimizing cross-contamination and maintaining consistent surface and tool conditions throughout the experiments.

Table 2. Combination of cutting parameters adopted.

Cutting tool	Cutting speed (V) [m/min]	Feed (f) [mm/tooth]	Axial depth of cut (ap) [mm]	Radial depth of cut (ae) [mm]	Oil [Yes/No]
1	65	0.095	3	2.4	No
2	40	0.095	2	2.4	Yes
3	40	0.095	2	2.4	No
4	65	0.115	2	1.5	Yes
5	80	0.095	4	1.5	Yes

During milling operations, the cutting edges exhibited several tool wear phenomena that affected the performance of the process. Fig. 2 shows some examples of tool wear, measured on the lateral cutting edges of the end mills. In addition to the expected increase in flank wear, a pronounced BUE formation was frequently observed. The presence of BUE significantly altered the cutting mechanics, leading to unstable chip formation, irregular force variations, and a local increase in thermal and mechanical loading on the cutting edge, making BUE a critical factor in the overall process quality. Therefore, the affected tools experienced an accelerated degradation process, often culminating in catastrophic wear, which caused pronounced deterioration of the surface quality of the machined workpiece.

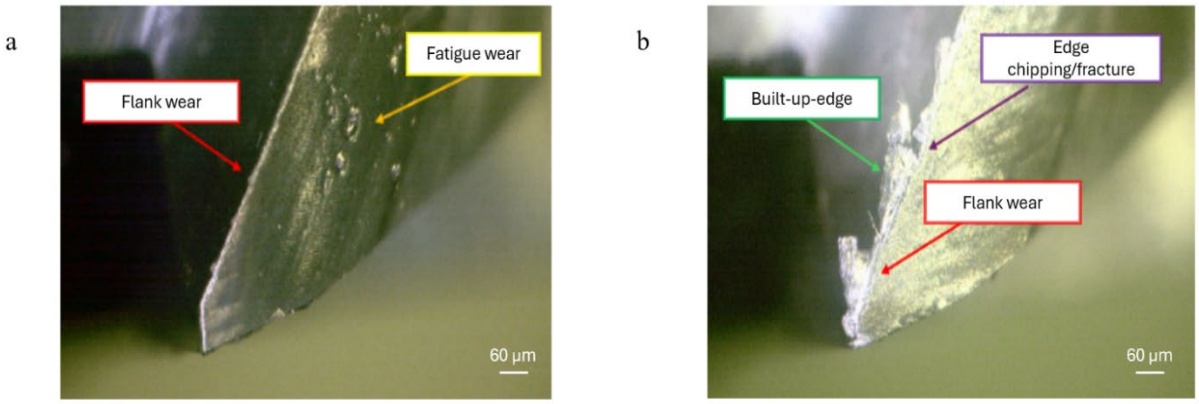

Fig. 2. Tool wear types: a) Flank wear and fatigue wear, b) Built-up edge and edge chipping/fracture.

The evolution of tool wear and the corresponding surface integrity of the machined workpiece were continuously monitored throughout the experiments, and the end of tool life was identified for each tool. During the experiments, surface defects such as tearing or material adhesion caused by BUE were systematically assessed through visual inspection, while flank wear was quantitatively measured at the end of each milling operation from the acquired images. The end of tool life was defined either when the flank wear reached the ISO 8688-2-defined limit or when surface quality was compromised due to BUE. These measurements provided the basis for defining the RUL variable, which quantifies the residual time before the tool reaches its predefined wear limit and must be replaced to ensure safe and stable machining operations.

Fig. 3a shows the evolution of the RUL, expressed as a percentage of cumulative cutting time, for each tool, highlighting pronounced variability among them. This discrepancy is largely attributed to differences in cutting conditions, such as the presence or absence of oil. Specifically, as shown in Fig. 3b, tools operating without oil generally exhibit a significantly reduced maximum cutting time, highlighting the strong influence of lubrication on tool performance and degradation.

Methodology

This section provides a background of the AI-based techniques adopted for the construction of a predictive model for RUL under variable cutting conditions. Vibration signals were cleaned and preprocessed to obtain the input dataset for the predictive models. Several deep learning algorithms and architectures were implemented, evaluated, and compared to identify the most effective predictive model.

Since the experiments involved different combinations of cutting parameters, the acquired vibration signals exhibit variable lengths. In addition, the two accelerometers employed in the setup operate at different sampling rates, further increasing the heterogeneity of the raw signals. Such discrepancies in signal duration and sampling characteristics make direct use of the full-length time series impractical for machine learning models, which typically require fixed-size inputs. To address this issue and enable consistent data representation across all operating conditions, a sliding-window segmentation strategy was adopted. Each vibration signal was partitioned into overlapping windows of fixed length, ensuring that every sample fed to the predictive model maintains identical dimensionality while preserving the temporal structure of the original measurements.

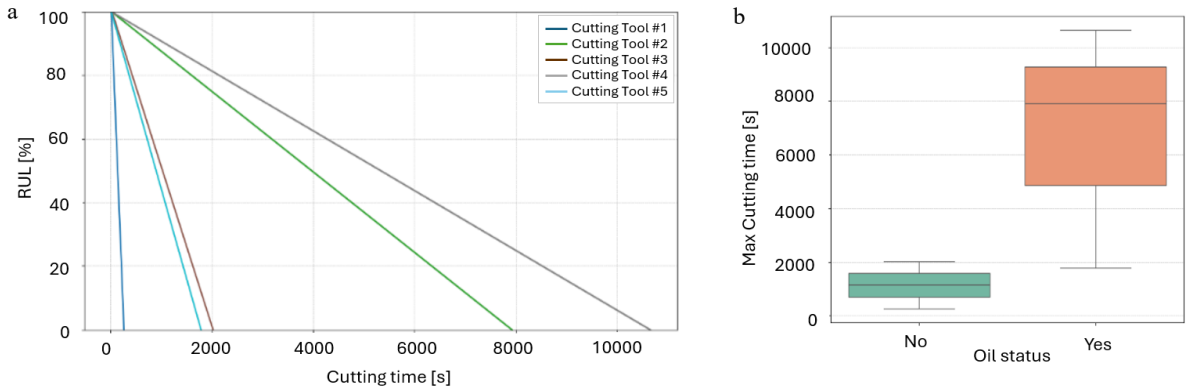

Fig. 3. Cutting tool degradation trend within the dataset. a) Temporal distribution of RUL across cutting tools and b) influence of lubrification on tool degradation.

Long Short-Term Memory (LSTM) networks and Convolutional Neural Networks (CNNs) were employed for the construction of the predictive model. LSTM network is a recurrent neural network (RNN)–based architecture designed to overcome key limitations of conventional RNNs, particularly in modeling long-range temporal dependencies. [20]. In standard RNNs, the model relies on a short-term memory, which corresponds to a rapidly decaying internal state updated at each time step. Because this memory is overwritten quickly, the network struggles to retain relevant information across longer temporal spans and requires extensive training to learn which information should be stored and for how long. This often results in vanishing gradient problems, inefficient learning, and degraded performance when long-range temporal dependencies are involved. LSTMs address these issues by introducing a more sophisticated memory mechanism, composed of explicit gating units that regulate the flow of information. These gates enable the network to preserve important features over extended sequences, selectively forget irrelevant content, and update its internal state efficiently.

Originally defined for pattern recognition within images, CNNs are one of the most impressive forms of artificial neural networks [21]. Their architecture consists of three types of layers: convolutional, pooling, and fully-connected layers. Convolutional layers constitute the core of a CNN and are responsible for extracting local features from the input data by connecting each neuron to a small part of the input data. This operation generates a set of feature maps, each highlighting specific patterns learned by the corresponding convolutional filter. Pooling layers operate directly on these feature maps, performing a downsampling procedure that reduces their spatial resolution and

consequently, the computational complexity while preserving the most salient information. Finally, fully-connected layers integrate the high-level features extracted by previous layers and combine them to produce the final output. Although CNNs were initially developed for computer vision tasks, their ability to learn spatially correlated structures has made them highly effective in a wide range of applications, including time-series analysis, signal processing, and industrial diagnostics [22].

In this work, a hybrid architecture combining the strengths of LSTM and CNN networks is proposed to construct an effective predictive model for RUL prediction. The performance of the hybrid LSTM–CNN model was assessed considering the three standard regression performance metrics listed in Table 3.

Table 3. Regression performance metrics.

Mean Absolute Error (MAE)	Root Mean Squared Error (RMSE)	R-squared (R^2)
$MAE = \frac{1}{N}\sum_{i=1}^{N}\lvert y_i - \hat{y}_i\rvert$	$RMSE = \sqrt{\frac{1}{N}\sum_{i=1}^{N}(y_i - \hat{y}_i)^2}$	$R^2 = 1 - \frac{\sum_{i=1}^{N}(y_i - \hat{y}_i)^2}{\sum_{i=1}^{N}(y_i - \underline{y}_i)^2}$
N: total number of samples y_i: true values $\hat{y}_i$: predicted values $\underline{y}$: average of the true values		

Results and Discussion

The vibration signals obtained during experimentation were used to develop a predictive model for estimating the RUL of the cutting tool when a CP-Ti plate is machined under variable cutting conditions. The preprocessing of the raw vibration signals and the development of the predictive model were carried out using the Python programming language and the PyTorch package [23]. From the acquired vibration data, the segments corresponding to the actual milling operation were first identified and isolated. Only the intervals in which the tool was effectively cutting the CP-Ti workpiece and completing a milling pass were retained, while idle or transient periods were removed.

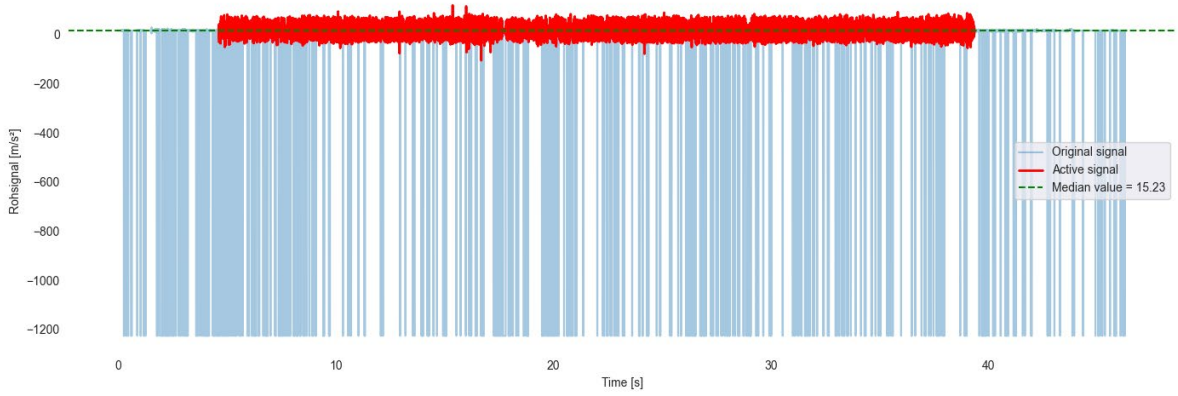

Fig. 4. Segment isolation from the spindle-vibration signal.

To achieve this, a combination of amplitude-based thresholds and temporal markers linked to the machine tool kinematics was applied. Fig. 4 shows an example of segment isolation from a vibration signal acquired by using the ToolVibe sensor.

A windowing strategy was implemented for the isolated segments to convert each variable-length signal into a structured set of fixed-length samples suitable for training the data-driven model. Specifically, each signal segment was divided into windows of 4096 samples with a step size of 2048

samples, corresponding to a 50% overlap. These windowed samples were subsequently fed into the neural architecture as input instances. Additionally, the available dataset was partitioned into three subsets for model training, validation, and testing, following a 70-15-15% split. The proposed neural architecture consists of a hybrid deep-learning architecture obtained by combining a bidirectional recurrent layer with a convolutional feature extractor, followed by a feature-fusion module. Fig. 5 illustrates the architecture of the developed predictive model. It was trained and tested on four input signal configurations: (a) radial spindle vibration, (b) three axes of the worktable independently, (c) three worktable axes jointly, and finally, (d) all available signals. This evaluation strategy allowed assessing the contribution of each signal source to the predictive performance of the model. The results obtained on the test set are reported in Table 4, with the best-performing configurations highlighted in bold.

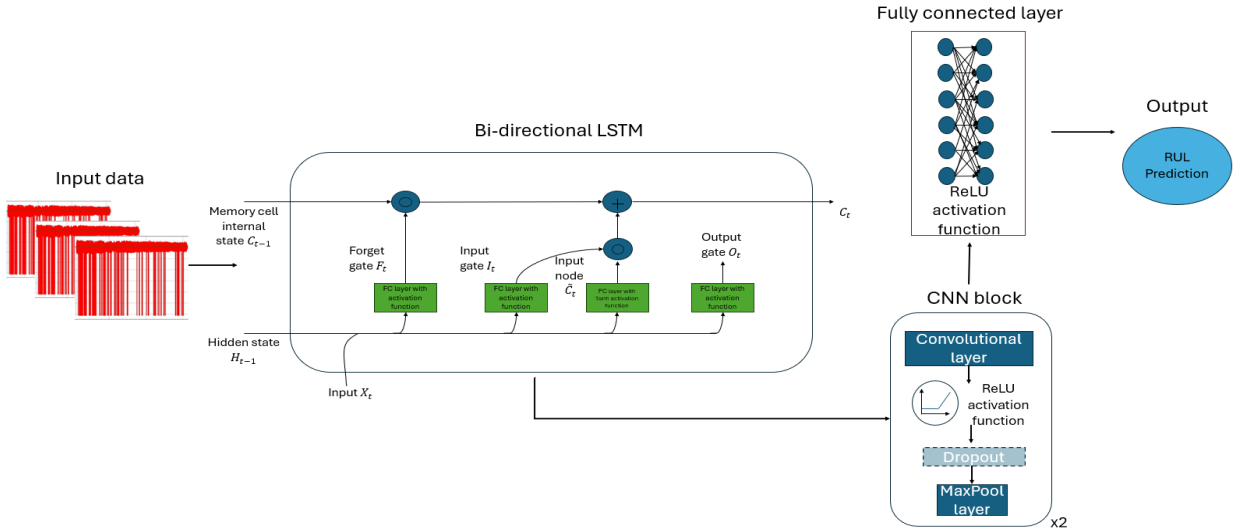

Fig. 5. Hybrid deep learning model architecture developed.

Table 4. Predictive results on the test set.

Input signals	MAE	RMSE	R^2
Radial spindle vibration	0.098	0.148	0.704
X-vibration worktable	0.111	0.151	0.692
Y-vibration worktable	0.084	0.123	0.798
Z-vibration worktable	0.218	0.256	0.120
Three-axis vibration worktable	0.065	0.093	0.883
All signals	**0.056**	**0.085**	**0.904**

Among the single-sensor inputs, the Y-axis vibration of the worktable achieves the best performance, with lower MAE and RMSE values and a higher R^2, immediately followed by the spindle-vibration signal. Although the Y-axis worktable vibration provides slightly better accuracy, the spindle-vibration signal represents a particularly attractive solution, as it is measured in the radial direction and can be acquired in a non-invasive manner, without requiring any modification or instrumentation of the worktable. This characteristic makes spindle vibration especially suitable for industrial applications, where ease of integration and minimal interference with the machining setup are critical. The best overall performance is obtained when all available signals are combined. This

highlights the benefit of sensor fusion, as the complementary information provided by different vibration sources improves the model's predictive capability and robustness.

To provide a more robust assessment of the model's generalization capability and to quantify performance variability, a 5-fold cross-validation procedure was additionally performed for each input configuration. For each fold, the model was trained from scratch, and the mean and standard deviation of MAE, RMSE, and R^2 were computed. Furthermore, 95% confidence intervals (CI) were estimated assuming normality of the performance distribution across folds. Results are presented in Table 5.

Table 5. 5-fold cross-validation results (mean ± standard deviation and 95% confidence intervals).

Input signals	MAE (mean ± std)	95% CI	RMSE (mean ± std)	95% CI	R^2(mean ± std)	95% CI
Radial spindle vibration	0.1186 ± 0.0117	± 0.0103	0.1753 ± 0.0109	± 0.0096	0.6311 ± 0.0460	± 0.0403
X-vibration worktable	0.0966 ± 0.0407	± 0.0357	0.1327 ± 0.0471	± 0.0412	0.7707 ± 0.1726	± 0.1513
Y-vibration worktable	0.1075 ± 0.0264	± 0.0231	0.1452 ± 0.0323	± 0.0283	0.7342 ± 0.1203	± 0.1055
Z-vibration worktable	0.1393 ± 0.0661	± 0.0579	0.1765 ± 0.0696	± 0.0610	0.5791 ± 0.3031	± 0.2657
Three-axis vibration worktable	0.0685 ± 0.0272	± 0.0238	0.0977 ± 0.0305	± 0.0267	0.8775 ± 0.0730	± 0.0640
All signals	0.0585 ± 0.0290	± 0.0254	0.0814 ± 0.0330	± 0.0579	0.9072 ± 0.0856	± 0.0750

The cross-validation analysis confirms the general trends observed in the fixed test set, while providing additional insight into the stability of each configuration. The model exploiting all available signals achieves the best overall performance in terms of mean MAE, RMSE, and R^2, thus confirming the benefit of sensor fusion. However, the associated standard deviations indicate a moderate variability across folds, suggesting a certain sensitivity to the specific data partitioning. Among the single-sensor configurations, the radial spindle-vibration signal exhibits comparatively low standard deviations for both MAE and RMSE, together with a limited dispersion in R^2 values. This behavior highlights its robustness and consistent predictive capability across different training subsets, further reinforcing its suitability for industrial deployment where reliability is critical. On the contrary, a reduced generalization stability is observed when worktable vibration signals are considered.

Additionally, a sensitivity analysis was performed by varying the window size while keeping all other parameters fixed, in order to systematically assess its impact on the predictive performance and to identify the most suitable configuration. Specifically, different window lengths were evaluated while maintaining a constant overlap ratio and identical training settings, so that any performance variation could be directly attributed to the window-size selection. Fig. 6 reports the MAE, RMSE, and R^2 values obtained on the test set for the considered window sizes by considering the radial spindle vibration and the Y-vibration worktable as input signals, respectively. For both signals, relatively low MAE and RMSE values and comparatively high R^2 were obtained with smaller window sizes. As the window size increases, the model performance deteriorates significantly, with a marked increase in prediction errors and a substantial drop in R^2. Based on these results, a window size of 4096 samples was selected for the final model configuration. This value ensures a balanced trade-off for both signal types, providing low MAE and RMSE together with a satisfactory R^2. For smaller window sizes, performance remains comparable but with slightly higher errors, whereas larger windows lead to a clear and consistent degradation of predictive accuracy.

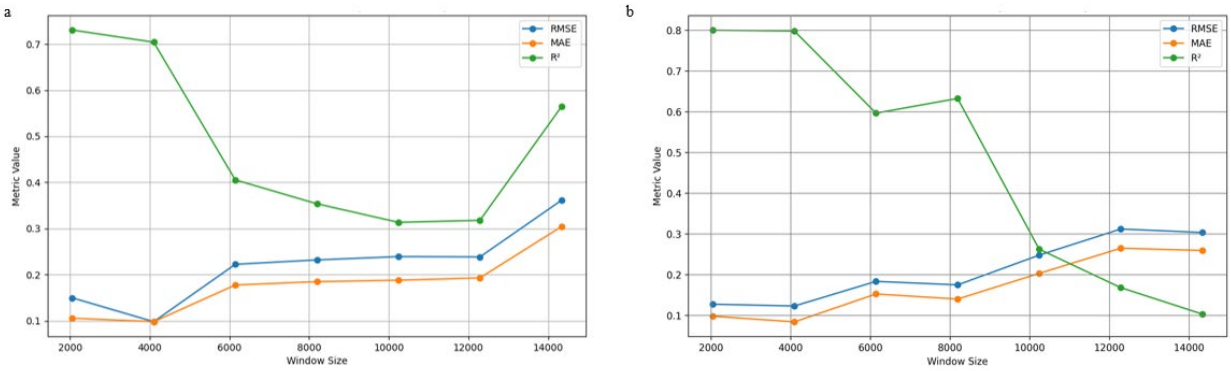

Fig. 6. Predictive performance to the selected window size for the two considered single-sensor configurations: (a) radial spindle vibration and (b) Y-axis worktable vibration.

Finally, an additional validation of the proposed model was carried out using the experiments performed with the sixth tool, under fully varying cutting conditions at each pass. This test represents a particularly challenging scenario, as none of the process parameters remain constant between consecutive passes. The results of this final validation are reported in Table 6.

Table 6. Predictive results under fully varying cutting conditions.

Input signals	MAE	RMSE	Mean Residual
Radial spindle vibration	**0.248**	**0.300**	**0.255**
X-vibration worktable	0.359	0.416	0.174
Y-vibration worktable	0.538	0.583	0.549
Z-vibration worktable	0.189	0.236	0.141
Three-axis vibration worktable	0.358	0.426	0.216
All signals	**0.220**	**0.290**	**0.163**

Even under these highly variable cutting conditions, the configuration exploiting all available signals still provides the best overall performance, achieving the lowest error metrics. However, it is worth noting that the model based solely on spindle vibration yields performance very close to that obtained with all signals combined, with comparable MAE and RMSE values, highlighting the high sensitivity of the spindle-vibration signal to process variations, even in strongly non-stationary conditions.

Conclusions and Future Work

This work investigated a vibration-based monitoring approach for milling tools under highly variable cutting conditions, with experimental validation carried out on CP-Ti, a material known for its challenging machinability. The main objective of the study was to identify and develop a predictive model based on a vibration signal capable of effectively capturing tool degradation and monitoring its RUL over time under variable cutting conditions. Accurate RUL prediction is of critical importance in industrial contexts, as it allows for optimized tool replacement strategies, reduced unplanned downtime, and improved process reliability, particularly when machining difficult-to-cut materials. Different vibration sources were analyzed and compared, including spindle and worktable sensors, in both single-sensor and multi-sensor configurations. The results showed that, while the combination of all available signals provides the highest overall accuracy, spindle vibration exhibits the best compromise between predictive performance and robustness under highly variable cutting conditions. Despite its non-invasive nature, this signal demonstrated a strong sensitivity to process

variations and delivered performance close to that of multi-sensor solutions, especially during the final validation on unseen tools and fully varying operating conditions.

Despite the encouraging results obtained in this study, the proposed approach has been validated on a limited number of cutting tools and workpiece materials, which represents an inherent limitation of the present work. Future research will focus on extending the proposed model to a wider range of variable operating conditions. In particular, the model will be validated using different tool types, characterized by varying materials and geometries, as well as across different workpiece materials. This extension will allow for a more comprehensive assessment of the model's generalization capability and robustness in heterogeneous industrial scenarios. Additionally, studies on uncertainty-aware RUL estimation will provide confidence bounds suitable for informed decision-making in industrial environments. Furthermore, optimised tool replacement strategies based on the predicted RUL will be developed by integrating RUL estimates into decision-making frameworks, with the aim of facilitating condition-based maintenance policies that optimise tool utilisation while minimising production downtime and associated financial expenditure.

Acknowledgement

This work contributes to the basic research activities of the WP9.6: "AI for Green" supported by the PNRR project FAIR - Future AI Research (PE00000013), Spoke 9 - Green-aware AI, under the NRRP MUR program funded by the NextGenerationEU. We thank Lennart Schinzel for his support with the experimental setup. We appreciate the Tool Vibe and support provided by REGO-FIX AG.

References

[1] Sarraf M, Rezvani Ghomi E, Alipour S, Ramakrishna S, Liana Sukiman N. A state-of-the-art review of the fabrication and characteristics of titanium and its alloys for biomedical applications. Biodes Manuf 2022;5:371–95. https://doi.org/10.1007/s42242-021-00170-3.

[2] Yang H, Luo S. Titanium products for everyday life by Panzhihua Story. Titanium for Consumer Applications, Elsevier; 2019, p. 13–25. https://doi.org/10.1016/B978-0-12-815820-3.00012-5.

[3] Campos F de O, Araujo AC, Kapoor SG. Experimental Comparison of Micromilling Pure Titanium and Ti–6Al–4V. J Micro Nanomanuf 2019;7. https://doi.org/10.1115/1.4043501.

[4] Proud L, Tapoglou N, Wika KK, Taylor CM, Slatter T. Role of CO2 cooling strategies in managing tool wear during the shoulder milling of grade 2 commercially pure titanium. Wear 2023;524–525:204798. https://doi.org/10.1016/j.wear.2023.204798.

[5] Srinivasa Reddy B, Pradeep Kumar M, Ashwin Jawahar S. Numerical and experimental validation of CP-Ti (Grade 2) under cryogenic condition. Mater Today Proc 2024. https://doi.org/10.1016/j.matpr.2024.01.046.

[6] Siahsarani A, Alinaghizadeh A, Azarhoushang B, Bayat M, Bösinger R. Sustainable and efficient cooling in titanium milling for dental applications: A study on supercritical CO2 + MQL with focus on tool wear and surface topography. Wear 2025;572–573:206051. https://doi.org/10.1016/j.wear.2025.206051.

[7] Assis JOM, Lauro CH, Pereira RBD, Brandão LC, Arruda ÉM, Davim JP. A Chip Formation Study of the Micro-Cutting of Commercially Pure Titanium. Metals (Basel) 2024;14:851. https://doi.org/10.3390/met14080851.

[8] Kumar J, Khamba JS. An experimental study on ultrasonic machining of pure titanium using designed experiments. Journal of the Brazilian Society of Mechanical Sciences and Engineering 2008;30. https://doi.org/10.1590/S1678-58782008000300008.

[9] Khan A, Maity K. Statistical modelling and machinability assessment of commercially pure titanium (CP-Ti) grade II: An experimental investigation. Measurement 2019;137:664–72. https://doi.org/10.1016/j.measurement.2019.02.018.

[10] Yedurkar DP, Schlech T, Sause MGR. A Systematic Review on Smart and Predictive Maintenance in Tool Condition Monitoring. IEEE Access 2025;13:106246–86. https://doi.org/10.1109/ACCESS.2025.3579204.

[11] Mohanraj T, Kirubakaran ES, Dinesh Kumar M, Naren ML, Suganithi Dharshan P, Mohamed I. Review of advances in tool condition monitoring techniques in the milling process. Meas Sci Technol 2024;35:092002. https://doi.org/10.1088/1361-6501/ad519b.

[12] Mohamed A, Hassan M, M'Saoubi R, Attia H. Tool Condition Monitoring for High-Performance Machining Systems—A Review. Sensors 2022;22:2206. https://doi.org/10.3390/s22062206.

[13] Assafo M, Langendoerfer P. Tool remaining useful life prediction using feature extraction and machine learning-based sensor fusion. Results in Engineering 2025;28:107297. https://doi.org/10.1016/j.rineng.2025.107297.

[14] Guo D, Liu Y, Sun L, Li G. A Novel Kolmogorov–Arnold Attention Allocation Network for Cutting Tool Remaining Useful Life Prediction. Applied Sciences 2025;15:11549. https://doi.org/10.3390/app152111549.

[15] Chen X, Cheng K. Cutting Tool Remaining Useful Life Prediction Using Multi-Sensor Data Fusion Through Graph Neural Networks and Transformers. Machines 2025;13:1027. https://doi.org/10.3390/machines13111027.

[16] Mohanraj T, Shankar S, Rajasekar R, Sakthivel NR, Pramanik A. Tool condition monitoring techniques in milling process — a review. Journal of Materials Research and Technology 2020;9:1032–42. https://doi.org/10.1016/j.jmrt.2019.10.031.

[17] Yaoguo M, Changfeng Y, Liang T, Minchao C, Junxue R, Ming L, et al. Research progress on intelligent monitoring of machining condition based on indirect method. Advanced Engineering Informatics 2025;67:103518. https://doi.org/10.1016/j.aei.2025.103518.

[18] Čuš F, Župerl U. Real-Time Cutting Tool Condition Monitoring in Milling. Strojniški Vestnik – Journal of Mechanical Engineering 2011;57:142–50. https://doi.org/10.5545/sv-jme.2010.079.

[19] Sobol' IM, Shukman BV. Random and quasirandom sequences: Numerical estimates of uniformity of distribution. Math Comput Model 1993;18:39–45. https://doi.org/10.1016/0895-7177(93)90160-Z.

[20] Hochreiter S, Schmidhuber J. Long Short-Term Memory. Neural Comput 1997;9:1735–80. https://doi.org/10.1162/neco.1997.9.8.1735.

[21] O'shea K, Nash R. An Introduction to Convolutional Neural Networks. n.d.

[22] Kiranyaz S, Avci O, Abdeljaber O, Ince T, Gabbouj M, Inman DJ. 1D convolutional neural networks and applications: A survey. Mech Syst Signal Process 2021;151:107398. https://doi.org/10.1016/j.ymssp.2020.107398.

[23] Paszke A, Gross S, Massa F, Lerer A, Bradbury J, Chanan G, et al. PyTorch: An Imperative Style, High-Performance Deep Learning Library 2019.